ACS APPLIED MATERIALS & INTERFACES

www.acsami.org

Research Article

Cell-Inspired Hydrogel Microcapsules with a Thin Oil Layer for Enhanced Retention of Highly Reactive Antioxidants

Jin-Ok Chu, Yoon Choi, Do-Wan Kim, Hye-Seon Jeong, Jong Pil Park, David A. Weitz, Sei-Jung Lee,* Hyomin Lee,* and Chang-Hyung Choi*

Cite This: *ACS Appl. Mater. Interfaces* 2022, 14, 2597−2604

Read Online

ACCESS | Metrics & More | Article Recommendations | Supporting Information

ABSTRACT: In nature, individual cells are compartmentalized by a membrane that protects the cellular elements from the surrounding environment while simultaneously equipped with an antioxidant defense system to alleviate the oxidative stress resulting from light, oxygen, moisture, and temperature. However, this mechanism has not been realized in cellular mimics to effectively encapsulate and retain highly reactive antioxidants. Here, we report cell-inspired hydrogel microcapsules with an interstitial oil layer prepared by utilizing triple emulsion drops as templates to achieve enhanced retention of antioxidants. We employ ionic gelation for the hydrogel shell to prevent exposure of the encapsulated antioxidants to free radicals typically generated during photopolymerization. The interstitial oil layer in the microcapsule serves as an stimulus-responsive diffusion barrier, enabling efficient encapsulation and retention of antioxidants by providing an adequate pH microenvironment until osmotic pressure is applied to release the cargo on-demand. Moreover, addition of a lipophilic reducing agent in the oil layer induces a complementary reaction with the antioxidant, similar to the nonenzymatic antioxidant defense system in cells, leading to enhanced retention of the antioxidant activity. Furthermore, we show the complete recovery and even further enhancement in antioxidant activity by lowering the storage temperature, which decreases the oxidation rate while retaining the complementary reaction with the lipophilic reducing agent.

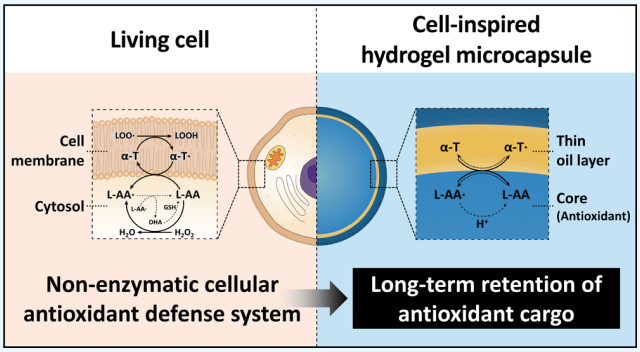

KEYWORDS: *droplet microfluidics, cell-inspired microcapsule, encapsulation, triple emulsion, reactive antioxidants*

INTRODUCTION

Living cells orchestrate various biochemical reactions to increase their vitality. These cells typically consist of an aqueous interior surrounded by a cell membrane that separates the cellular elements from the surrounding environment. The cellular membrane is semipermeable and stimulus-responsive, protecting the cells from the toxins in the local environment while regulating the composition of the interior to effectively coordinate a series of intracellular reactions within the subcellular compartments and perform central functions.[1] For instance, organelles in cells often generate reactive oxygen species (ROS) during respiration or photosynthesis, which can cause severe damage to proteins, lipids, carbohydrates, and DNA, resulting in oxidative stress of cellular components.[2] To counteract the oxidative stress, cells are inherently equipped with an antioxidant defense system in which nonenzymatic low molecular weight metabolites, such as ascorbate, glutathione, and α-tocopherol, functionally interplay in the cellular protective mechanism.[3] Translation of these synergistic complementary reactions occurring in actual cells into cellular mimics can potentially lead to the design of advanced microcarriers that enable long-term retention and effective delivery of reactive and thus sensitive antioxidants; however, a similar conceptual idea has not been presented.

Recent advances in experimental techniques have led to preparation of synthetic cellular models that incorporate the imperative aspects of living cells.[4−8] In particular, droplet microfluidics allow precision control over fluids for preparation of monodisperse multiphase emulsions, which serve as ideal templates to create polymersomes,[9−11] liposomes,[12,13] microgels,[14,15] and core−shell type microcapsules.[16−18] As microfluidics allow high throughput production of microparticles with tunable composition and structure, considerable attention and effort have been devoted to exploit the ability to encapsulate and retain various cargoes in these multicompartmental microcarriers with high encapsulation efficiency.[19,20] For instance, double emulsions, drops that contain

Received: October 27, 2021
Accepted: December 23, 2021
Published: January 4, 2022

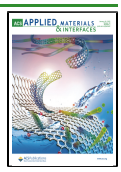

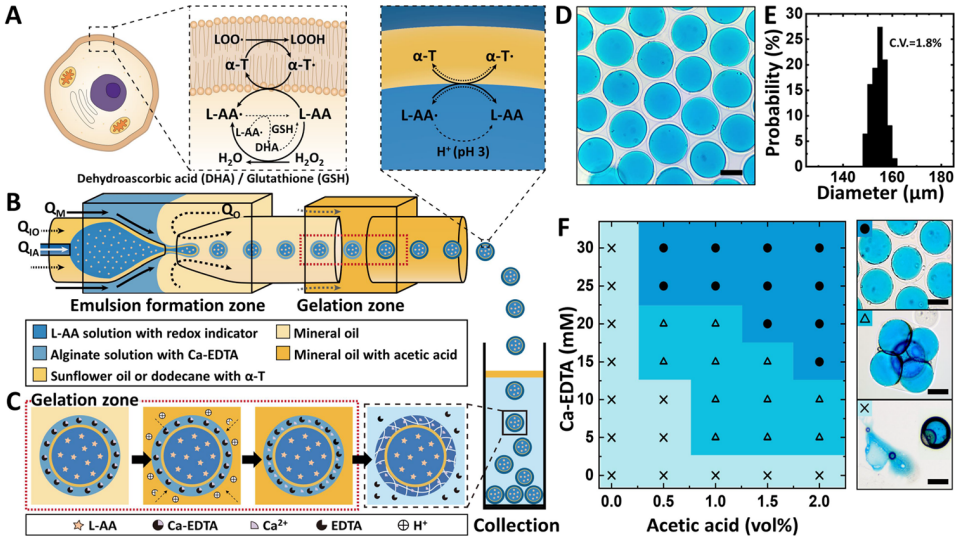

Figure 1. Microfluidic production of cell-inspired hydrogel microcapsules. (A) Schematic showing a nonenzymatic cellular antioxidant defense system; (B) schematic showing a glass capillary microfluidic device for the production of water-in-oil-in-water-in-oil (W/O/W/O) triple emulsion drops, which transform into hydrogel microcapsules via ionic gelation. The resulting hydrogel microcapsules are directly collected in water without extra washing step. (C) Schematics showing the detailed sequential procedures for the preparation of ionic gelation-based hydrogel microcapsules. (D) Bright-field micrograph and (E) corresponding size distribution plot showing the collected monodisperse hydrogel microcapsules in water. We carried out a quantitative analysis for size distribution using an entire population of 100 particles. (F) Phase diagram showing microcapsule formation as a function of acetic acid ($C_{acetic\ acid}$) and Ca-EDTA ($C_{Ca\text{-}EDTA}$) concentration; maximum solubility of acetic acid in mineral oil is around 2%. The bright-field micrographs show the complete gelation (solid circle), partial gelation (open triangle), and no gelation (cross), respectively. Scale bars represent 100 μm.

an additional smaller drop inside, have been used as templates for production of various types of stimulus-responsive microcapsules,[21,22] enabling encapsulation and externally triggered release of hydrophilic and hydrophobic cargoes embedded in each compartment, depending on their solubility (i.e., polarity).[23−25] However, the variability in the selection of materials as well as compartments that can be modulated for double emulsions limits the simultaneous fulfillment of all the sophisticated demands such as biocompatibility, long-term retention, and stimulus-responsiveness. Such double emulsions have been used to induce self-assembly of either synthetic polymers or phospholipids into a bilayer structure to result in polymersomes and liposomes.[26,27] While these vesicles resemble the cells' membrane structure and have been widely utilized for efficient delivery of therapeutics and active ingredients as well as for mimicking the complex biochemical reactions occurring inside cells,[28,29] they are both inherently less stable compared to microcapsules commonly prepared by solidification of the middle phase via the photopolymerization process as they are driven by relatively weak hydrophobic interactions. Alternatively, triple emulsion drops with an additional compartment have recently been proposed to prepare microcapsules with an interstitial layer that separates the innermost drop containing the cargo of interest from the capsule shell, enabling successful encapsulation and retention of various cargoes as well as smart release of these cargoes, triggered via diverse stimuli.[30−33] While the presence of an interstitial oil layer in a triple emulsion drop allows effective isolation of the cargo containing innermost aqueous drop from the surrounding environment until external stimuli are applied, it is still difficult to achieve long-term retention of reactive cargoes such as antioxidants, as they are vulnerable to an oxidizing environment including light, oxygen, moisture, and temperature.[34] This precludes the broader applicability of microfluidic technologies in the delivery of antioxidants due to low efficacy. Moreover, the photopolymerization process most widely used to prepare the solidified shell in microcapsules often generates free radicals, which facilitate the oxidation and further decrease the efficacy. Therefore, there remains a need for a microcapsule design that simultaneously allows long-term retention of antioxidants as well as triggered release via diverse stimuli.

In this study, we present a new hydrogel microcapsule design to achieve long-term retention of highly reactive antioxidant cargoes, inspired by the cellular protective mechanism. We use triple emulsion drops with a thin interstitial oil layer that separates the aqueous core containing reactive antioxidants from the hydrogel prepolymer phase, resulting in monodisperse alginate hydrogel shelled microcapsules via ionic gelation; this prevents exposure of the encapsulated antioxidants to free radicals typically generated during photopolymerization. In addition, we show that the interstitial oil layer in the microcapsule serves as a versatile compartment in which the antioxidant can be efficiently and stable stored in the aqueous core until osmotic pressure is imposed to destabilize the oil layer and release the cargo on-demand. Moreover, by incorporating a lipophilic reducing agent within this oil compartment, we induce a synergistic and complementary reaction with the encapsulated antioxidant across the water/oil interface to yield long-term retention of the antioxidant activity, similar to the nonenzymatic antioxidant defense system in cells. Furthermore, we demonstrate the facile recovery and even further enhancement in the antioxidant activity upon lowering of the storage temperature, which reduces the oxidation rate while retaining the complementary reaction with the lipophilic reducing agent.

https://doi.org/10.1021/acsami.1c20748
ACS Appl. Mater. Interfaces 2022, 14, 2597−2604

RESULTS AND DISCUSSION

To realize the nonenzymatic antioxidant defense system of actual cells in a cellular mimic, we prepare hydrogel microcapsules with an interstitial oil layer that separates the innermost aqueous drop containing the model antioxidant, L-ascorbic acid (L-AA), from the capsule shell. While the presence of the interstitial oil layer allows effective isolation of L-AA from the surrounding environment, the incorporation of α-tocopherol (α-T) in the oil layer additionally protects the encapsulated L-AA from oxidation by external factors (e.g., oxygen, pH, and temperature), similar to the α-T embedded within the hydrophobic domain of the cellular membrane in actual cells, as schematically illustrated in Figure 1A. In cells, the cellular membrane not only serves as a physical barrier but also provides a compartment for the hydrophobic α-T to interact in a complementary fashion with the L-AA encapsulated in the aqueous core to retain its activity. While bilayer structured vesicles, including polymersomes and liposomes, better mimic the cells' membrane structure, we instead focus on analogous hydrogel microcapsules to replace the hydrophobic domain with an oil layer while enhancing the overall stability of the microcarrier.

To produce these microcapsules, we utilize a triple emulsion-based microfluidic approach as shown in Figure 1B. Triple emulsion drops serve as templates to produce hydrogel microcapsules with an interstitial oil layer and are prepared using a glass capillary microfluidic device; the device fabrication procedure is detailed in the Supporting Information. After device fabrication, an aqueous solution (innermost aqueous phase, Q_{IA}) containing L-AA and a redox indicator, erioglaucine disodium salt (blue), is supplied through a small tapered capillary. To ensure the initial stability of the L-AA, the pH of the innermost aqueous core is kept at 3[35] and a redox indicator is used to probe the oxidation state of L-AA; blue color (no color change) implies successful retention of the L-AA activity, while color loss (transparent) indicates their oxidation. We choose sunflower oil, which inherently contains 0.05% α-T[36] as the inner oil phase (Q_{IO}), and it is supplied through the injection capillary along with the innermost aqueous phase (Q_{IA}) to form a periodic stream of large aqueous blobs in the oil phase due to the preferential wetting of the oil phase onto the wall of the hydrophobically treated injection capillary. This surface treatment facilitates the formation of a thin lubrication oil layer between the innermost aqueous blobs and the wall of the injection capillary. Next, 2% alginate solution (middle phase, Q_M) containing calcium disodium EDTA (Ca-EDTA) is supplied through the interstices between the injection capillary and the square capillary, from the same direction. The triphasic coaxial flows are emulsified near the entrance of the collection capillary by shearing of the outer oil phase (2% Span80 in mineral oil, Q_O), forming highly uniform triple emulsion drops with a thin oil layer. These emulsion drops flow through an additional square capillary where the outer oil phase containing acetic acid is supplied to induce ionic gelation. The acetic acid dissolved in the mineral oil phase diffuses into the alginate solution phase (Q_M) and is followed by release of calcium ions (Ca^{2+}) by dissociation of Ca-EDTA to form an alginate hydrogel shell,[37] as shown in Figure 1C. Then, the resulting microcapsules in the oil phase are transferred into an aqueous buffer solution; the oil phase is readily separated from the microcapsules due to its lower density and to the preferential wetting of the hydrogel shell with the aqueous buffer solution (estimated production yield of the microcapsules is approximately 300 capsules/s). By tuning the inner oil phase flow rate (Q_{IO}) and the innermost aqueous phase flow rate (Q_{IA}), monodisperse microcapsules can be prepared in dripping regime, as evidenced by the micrograph and the size distribution plot of Figure 1D,E and the phase diagram of Figure S1. Microcapsules with the same size but with different core−shell ratios can also be prepared by controlling the flow rates of the innermost aqueous phase flow rate while keeping the overall inner phase flow rate as well as the outer phase flow rate constant (Figure S2). In addition, we observe negligible color variance within the innermost core of the microcapsules, indicating that L-AA is successfully encapsulated without oxidation during the fabrication process. Furthermore, as the stable formation of an alginate-based hydrogel shell in microcapsules relies on the concentration of acetic acid ($C_{acetic\ acid}$) and Ca-EDTA ($C_{Ca\text{-}EDTA}$), we monitor the ionic gelation behavior in the capillary device and prepare a phase diagram as shown in Figure 1F; the sold circles, open triangles, and crosses in the diagram each refer to complete gelation, partial gelation, and no gelation, respectively. For low $C_{Ca\text{-}EDTA}$ and $C_{acetic\ acid}$, gelation does not occur due to depletion of Ca^{2+} ions (crosses), while partial gelation and thus incomplete capsule formation appear for slightly higher $C_{Ca\text{-}EDTA}$ (over 5 mM) with excess $C_{acetic\ acid}$ (1−2%, open triangles). As $C_{Ca\text{-}EDTA}$ is further increased, the Ca^{2+} ion concentration becomes sufficient to induce complete gelation, resulting in stable formation of the hydrogel microcapsules (solid circles). By contrast, preparation of analogous microcapsules with a poly(ethylene glycol) (PEG) hydrogel shell via UV-induced free radical polymerization clearly reveals that the ionic gelation process is required as L-AA within the PEG microcapsule is readily oxidized to an ascorbyl radical due to generation of free radicals during the polymerization process. Visual comparison between the two sets of PEG microcapsules with and without L-AA shows that the free radicals reduce the redox indicator, as evidenced by the dramatic difference in the colorimetric response shown in the sets of micrographs in Figure S3; if all the conditions are not satisfied (e.g., in the absence of the L-AA), the color originating from the redox indicator does not change. Overall, these results show that the most commonly used photopolymerization approach to produce hydrogel microcapsules is incompatible due to generation of free radicals and that ionic gelation is more suitable to effectively encapsulate antioxidants within the hydrogel microcapsules.

To quantitatively assess the effective retention of L-AA in the hydrogel microcapsules with a thin oil layer, we prepare microcapsules and store them in 14% sucrose solution (430 $mOsmol kg^{-1}$) whose osmolarity is matched with that of the innermost aqueous phase containing 1% L-AA at room temperature (20 °C) (Figure 2A). As the presence of an interstitial oil layer within the hydrogel microcapsule allows isolation of the innermost aqueous phase from the surrounding environment until osmotic pressure is imposed to destabilize the oil layer, the activity of the encapsulated L-AA can be evaluated at different time intervals. The alginate hydrogel shell in the microcapsules has an estimated mesh size of 5 nm,[38] which is thus larger than the hydrodynamic diameter of L-AA, which is approximately 0.3 nm.[39] This enables determination of the L-AA activity upon destabilization of the thin oil layer via transfer into deionized (DI) water, which induces osmotic stress. Collection of the released L-AA in separate vials

https://doi.org/10.1021/acsami.1c20748
ACS Appl. Mater. Interfaces 2022, 14, 2597−2604

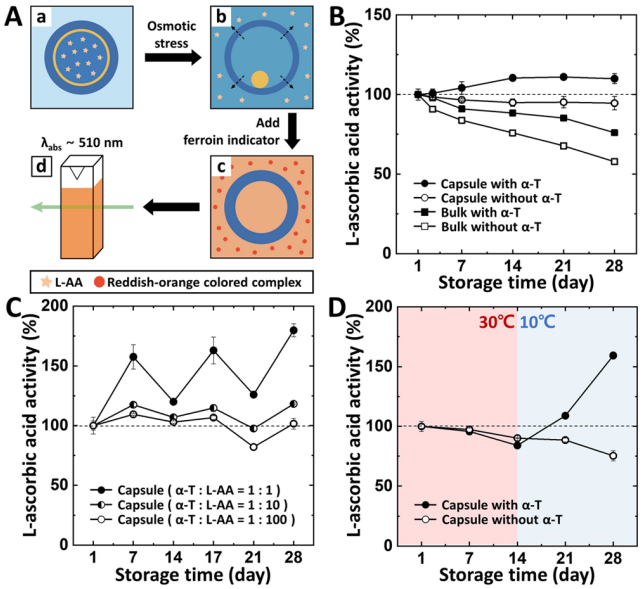

Figure 2. Quantitative analysis of retention capability of antioxidants in microcapsules. (A) Schematics showing a sequential procedure to probe the L-AA activity by extracting samples from the microcapsules with varying storage periods. (B) Plot showing retention capability of L-AA kept under varying storge conditions; microcapsules with (solid circle) or without α-T (open circle) and bulk with (solid square) or without α-T (open square). (C) Plot showing retention capability of L-AA in microcapsules with different molar ratios between L-AA and α-T (α-T/L-AA). (D) Plot showing the regeneration capability of L-AA with variation in the storage temperature from 30 to 10 °C. We carried out quantitative analysis for retention capability through a total of five batches; consistent results were obtained in the experiment repeated three times.

followed by addition of a mixed reagent containing Fe^{3+} and 1,10-phenanthroline allows measurement of the L-AA activity as shown in the schematics of Figure 2A; L-AA reduces Fe^{3+} to Fe^{2+}, which subsequently forms a reddish-orange colored complex with 1,10-phenanthroline for detection via UV−vis spectroscopy ($\lambda_{abs} \sim 510$ nm).[40]

While we initially anticipated that utilizing sunflower oil in the microcapsule could potentially prevent oxidation of L-AA by the α-T inherently present in sunflower oil, we instead find that the L-AA encapsulated within these microcapsules is readily oxidized in a short period, as evidenced by the rapid decay in L-AA activity with respect to storage time shown in the plot of Figure S4. This is presumably due to oxidation of α-T in the sunflower oil prior to usage, as an aliquot amount of fresh α-T addition in the sunflower oil layer significantly suppresses the reduction of L-AA activity. Therefore, to avoid such confusion originating from the uncertain contribution of α-T in the sunflower oil layer, we instead use hydrocarbon oil such as dodecane for the thin oil layer to clearly verify the interaction between α-T and L-AA and their effect on L-AA activity.

To achieve this, we prepare two sets of hydrogel microcapsules with and without α-T in the oil layer comprising dodecane and compare their L-AA activity with the analogous bulk experiment results.[41,42] In the bulk test, L-AA solution is kept in two separate amber glass vials each with an oil layer on top but with only one containing the same concentration of α-T in the oil layer. Surprisingly, we find that the L-AA activity of the microcapsules with the α-T-containing dodecane layer (solid circle) is retained for a month and even exceeds the original value as shown in the L-AA activity plot of Figure 2B. By contrast, microcapsules without α-T (open circle) exhibit slight reduction in L-AA activity to 94.6 ± 4.25% after a month, indicating that L-AA oxidation cannot be completely prevented without the presence of α-T and that the interplay of α-T and L-AA is essential for efficient retention of L-AA in the microcapsules. Further comparison of the L-AA activity with bulk conditions (both with and without α-T) clearly reveals that L-AA readily oxidizes upon exposure to oxygen. Moreover, this microencapsulation strategy not only reduces the exposure of L-AA to the external oxidizing environment but also facilitates the interfacial interaction with α-T due to a higher surface-to-volume ratio as compared to bulk.

To further investigate how the molar ratio of α-T and L-AA affects the L-AA activity, we prepare sets of microcapsules incorporating the same amount of L-AA but with variation in the α-T concentration of the oil layer as shown in Figure 2C; the molar ratios of α-T to L-AA range from 1:1 and 1:10 to 1:100, respectively. We observe the highest value of L-AA activity at a 1:1 molar ratio, consistent with the reported reaction stoichiometry of 1:1 between α-T and L-AA. The stoichiometrically matched condition allows the optimal interaction between α-T and L-AA across the water/oil interface, leading to exceptionally high L-AA activity over extended periods of time. In addition, we also observe zigzag trends in the activity value under all conditions tested, implying the consistent interplay between the two antioxidants, as reported by others in bulk emulsification.[43] For simplicity, we denote the L-AA-encapsulated hydrogel microcapsules with a thin oil layer comprising dodecane as microcapsules, and when α-T is included in the oil layer, the molar ratio of α-T to L-AA is set to 1:1 hereafter unless specified.

To clearly verify the origin of this pronounced increase in L-AA activity observed in microcapsules with α-T, we prepare a separate set of experiments in which microcapsules with and without α-T are exposed to elevated temperature of 30 °C. Monitoring the L-AA activity over time reveals that increasing the storage temperature leads to rapid oxidation of the L-AA in both microcapsules regardless of the existence of α-T, as shown in Figure 2D. This is possibly due to higher oxidation kinetics of both antioxidants at 30 °C, as reported previously;[44] the oxidation rate of L-AA is much faster than the reduction given by the α-T. However, when the storage temperature is reduced to 10 °C, microcapsules with the α-T exhibit a dramatic increase in the L-AA activity compared to the α-T deficient analogue. This result indicates that the L-AA reduction by interaction with α-T overcomes the oxidation rate at lower temperature, increasing the L-AA activity. Overall, our proposed cell-inspired microcapsule design not only allows effective encapsulation of antioxidants but also regenerates them through the synergistic interplay between two antioxidants, L-AA and α-T, respectively.

To more completely assess the long-term retention of L-AA activity in the proposed microcapsules, we employ the cellular oxidative stress model induced by hydrogen peroxide (H_2O_2) in human epithelial Caco-2 as well as fibroblast NIH-3 T3 cells; we note that both cell lines have been extensively studied as common major cell types to investigate the physiological functions of epithelial cells and fibroblasts. For this purpose, we additionally prepare two sets of L-AA-encapsulated microcapsules with and without α-T and compare their L-AA activity at the cellular level with the bulk experiment (without

https://doi.org/10.1021/acsami.1c20748
ACS Appl. Mater. Interfaces 2022, 14, 2597−2604

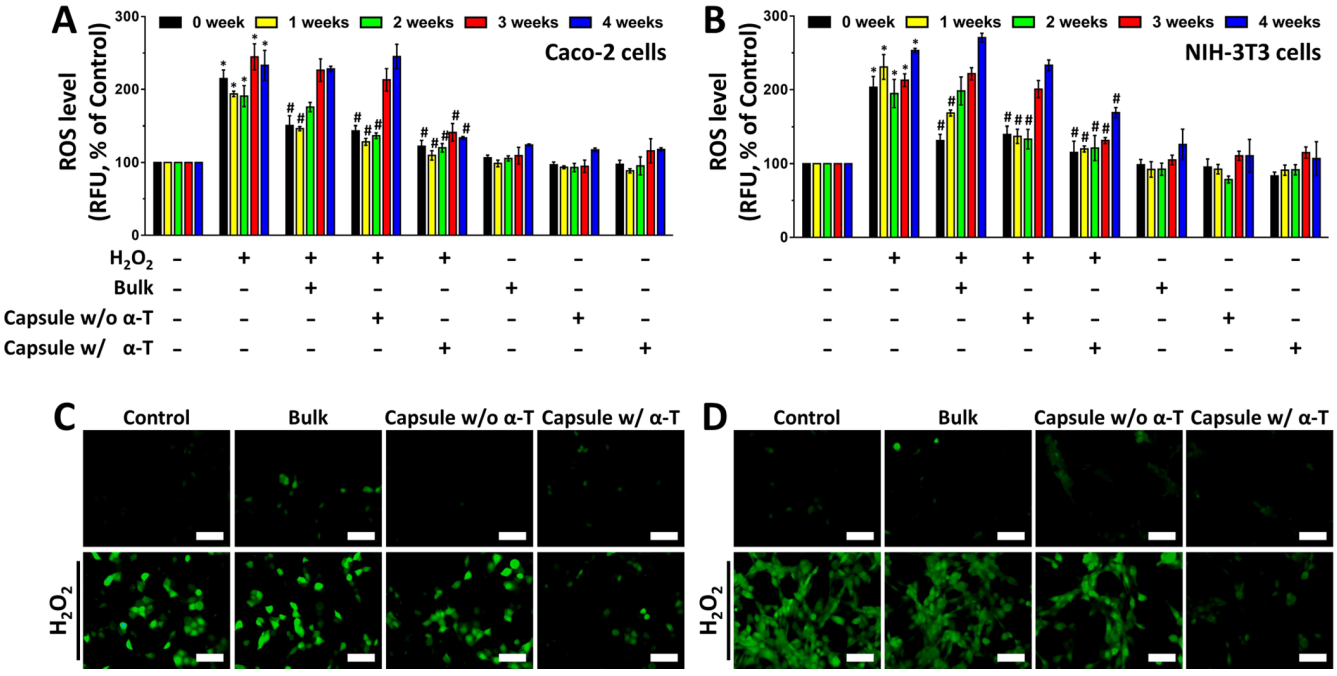

Figure 3. Investigation of antioxidant retention capability using cellular oxidative stress models. Plots showing the level of ROS production in (A) Caco-2 and (B) NIH-3 T3 cells treated with L-AA-encapsulated microcapsules with and without α-T prior to H_2O_2 exposure for 4 h are shown. Data represent mean ± S.E. $n = 4$. *$p \leq 0.01$ vs control. #$p \leq 0.05$ vs H_2O_2 alone. RFU, relative fluorescence units. ROS production (green) at 4 weeks in (C) Caco-2 and (D) NIH-3 T3 cells was visualized by confocal microscopy. Scale bars represent 100 μm (original magnification × 100). $n = 4$.

an upper oil layer); the L-AA released from the microcapsules and the ones kept in the amber glass vials (bulk) are collected from each sample condition and evaluated every week for 1 month. We measure the level of ROS 30 min after addition of 100 μM H_2O_2 by using a cellular ROS indicator, a chloromethyl derivative of H_2DCFDA (CM-H_2DCFDA), in the spectrofluorometer and separately monitor the retention of trapped ROS inside the cell via fluorescence microscopy. We find that the production of ROS provoked by H_2O_2 in the Caco-2 (Figure 3A) and NIH-3 T3 cells (Figure 3B) is effectively suppressed in all conditions tested for 1 week. After 2 weeks, however, the bulk L-AA fails to scavenge the ROS due to oxidative stress imposed by the external environments. By contrast, microcapsules with α-T exhibit sustainable antioxidative effect with small variance in the ROS level for more than 3 weeks. Also, microcapsules without α-T cannot prevent L-AA oxidation and do not show noticeable inhibitory effect on ROS production after 3 weeks, confirming that the presence of α-T in the microcapsule is indeed critical for securing long-term retention of L-AA activity.

The potential of these microcapsules with α-T is further verified by the direct visualization of the corresponding cell behavior. Both Caco-2 cells and NIH-3 T3 cells are stained with a fluorescent CM-H_2DCFDA, which passively diffuses into cells, where its acetate groups are removed by intracellular esterases and oxidation occurs within the cell to yield a fluorescent adduct. We observe that only microcapsules with α-T exhibit negligible green fluorescence signal intensity, implying that the ROS is effectively suppressed by the large portion of the active L-AA remaining that is successfully enclosed for extended periods of time as shown in Figure 3. These results are consistent with the results shown in Figure 2 and further confirm the efficacy of the cell-inspired microcapsule with a thin oil layer for enhanced retention of antioxidants.

CONCLUSIONS

In summary, cell-inspired hydrogel microcapsules with an interstitial oil layer containing lipophilic reducing agents are prepared using triple emulsion drop-based microfluidics. Unlike the conventional photopolymerization method, which generates free radicals, ionic gelation of the hydrogel shell in microcapsules allows successful encapsulation of antioxidants without loss of activity. In addition, the interstitial oil layer in the microcapsule acts as an effective diffusion barrier, allowing efficient encapsulation of small antioxidants within the porous hydrogel shell and providing an adequate pH microenvironment to retain their activity. Moreover, by incorporating the lipophilic reducing agent (α-tocopherol) within the thin oil layer, we show that enhanced retention of antioxidant activity can be achieved by the complementary reaction of α-tocopherol with the antioxidant at the water/oil interface, similar to the nonenzymatic antioxidant defense system in cells. Furthermore, we demonstrate that the loss of antioxidant activity can be fully recovered and even further enhanced by simply lowering the storage temperature via reduction in the rate of oxidation. We envision that these microcapsules will establish a new pathway in long-term storage and programmable release of highly reactive and sensitive cargoes, which has increasing demand in various fields, including cosmetics, foods, and pharmaceutics.

EXPERIMENTAL SECTION

Materials. L-Ascorbic acid (99%), (±)-α-tocopherol (synthetic, ≥96% (HPLC)), hydrochloric acid solution (1.0 N, BioReagent, suitable for cell culture), erioglaucine disodium salt (redox indicator), alginic acid sodium salt, calcium chloride, ethylenediaminetetraacetic

https://doi.org/10.1021/acsami.1c20748
ACS Appl. Mater. Interfaces 2022, 14, 2597−2604

acid disodium salt dihydrate (ACS reagent, 99.0−101.0%), poly(vinyl alcohol) (PVA, Mw 13,000−23,000, 87−89% hydrolyzed), synperonic F108 (poly(ethylene glycol)-block-poly(propylene glycol)-block-poly(ethylene glycol), nonionic surfactant, Mw 14,600), mineral oil, *n*-dodecane, span 80 (Sorbitan monooleate, viscosity 1000−2000 mPa.s (20 °C)), sucrose, polyethylene glycol diacrylate (PEGDA, average Mn 700), 2-hydroxy-2-methylpropiophenone (97%, photoinitiator), 1,10-phenanthroline monohydrate, ammonium iron(III) sulfate dodecahydrate, and trichloro(octadecyl) silane were purchased from Sigma-Aldrich. 2-[Methoxy(polyethyleneoxy)propyl]trimethoxyl silane was purchased from Gelest. DI water (EXL 18.2 MΩ·cm at 28 °C) was used for all aqueous solutions. Square glass capillaries with an inner diameter of 1.05 mm were purchased from Atlantic International Technology (A.I.T.), and cylindrical glass capillaries with an inner diameter of 0.58 mm and outer diameter of 1.00 mm were purchased from World Precision Instruments Inc. (W.P.I.); 5 min epoxy (Devcon) was used for assembling the glass capillary microfluidic devices. A microscope slide (3 × 1 in, DURAN) and cover glass (Deckglaser) were used to fabricate a custom-made chamber for micropipette aspiration.

Methods. *Fabrication of a Glass Capillary Microfluidic Device and Its Operation.* We prepare an injection capillary by tapering a 580 μm inner diameter circular (cross-section) glass capillary to a 100 μm inner diameter; to make the inner wall hydrophobic, we dip the capillary to trichloro(octadecyl) silane for 10 min and subsequently wash it with ethanol. We insert the injection capillary into a square capillary whose inner width (1.05 mm) is slightly larger than that of the outer diameter of the injection capillary (1 mm). Next, we prepare a small tapered glass capillary (20 μm outer diameter) by pulling a cylindrical capillary; this capillary is inserted into the injection capillary for coinjection of two immiscible fluids (innermost and inner phases). Finally, a collection capillary tapered (inner diameter of orifice: 350 μm) is inserted into the square capillary from the other end; we also treat this collection capillary with trichloro(octadecyl) silane to make the capillary wall hydrophobic. During drop generation, the volumetric flow rate is precisely controlled with syringe pumps (Legato100, KD Scientific) and the production of emulsion drops is observed using an inverted fluorescence microscope (Eclipse Ti2, Nikon) equipped with a high-speed camera (MINI UX 50).

Characterization of Hydrogel Microcapsules. An inverted fluorescence microscope (Eclipse Ti2, Nikon) equipped with a CCD camera (sCMOS Zyla, Andor) was used to observe the resulting hydrogel microcapsules, and image analysis of the particles was performed using the ImageJ (National Institute of Health) and NIS-Elements (Nikon) software programs. The time-dependent release patterns upon applying external stimuli was observed and characterized by confocal microscopy (SP-5, Leica). Osmolarity of all aqueous solutions is measured using a freeze point osmometer (Osmomet 3000, Gonotec) before use.

Sample Preparation for Quantitative Analysis of L-AA Activity. To prepare each capsule sample consistently, we collected the same aliquot of capsule suspension (in mineral oil, 0.5 mL) for 3 min to retain the same average number (approximately 54,000 capsules) of the microcapsules in a vial containing DI water; the microcapsules were dispersed in the water due to the higher density of the microcapsule than water, while we thoroughly removed the mineral oil with a pipette.

Intracellular Reactive Oxygen Species (ROS) Detection. To quantify the intracellular ROS levels, the cells treated with 10 mM CM-H_2DCFDA (Thermo Fisher Scientific, Waltham, MA, USA) were rinsed twice with ice-cold phosphate-buffered saline (PBS) and then scraped. A 100 μL cell suspension was loaded into a 96-well plate and examined by using a luminometer fluorescent microplate reader (SPARK, Seestrasse, Männedorf, Switzerland) at excitation and emission wavelengths of 485 and 535 nm, respectively.

Cell Culture. Human intestinal epithelial Caco-2 cells and mouse embryonic fibroblast NIH-3 T3 cells were purchased from the American Type Culture Collection (ATCC, Manassas, VA, USA) and were grown at 37 °C in 5% CO_2 in Dulbecco's Modified Eagle Medium (DMEM, Thermo Fisher Scientific, Waltham, MA, USA) complemented with 10% FBS and antibiotics (10 units/mL penicillin G and 10 μg/mL streptomycin). For the experiments, cells were seeded on a culture plate at 1×10^5 cells/cm^2 and maintained until confluent. Following incubation, the cells were washed twice with PBS and then maintained in serum-free DMEM at least 24 h, including all supplements and indicated agents.

Statistical Analysis. Data are represented as mean value ± standard errors (S.E.). Statistical significance was analyzed by one-way analysis of variance (ANOVA) in SPSS 16 software (IBM Corp, Armonk, NY, USA). $p < 0.05$ is considered significant.

■ ASSOCIATED CONTENT

Supporting Information

The Supporting Information is available free of charge at https://pubs.acs.org/doi/10.1021/acsami.1c20748.

Phase diagram showing flow patterns in a microfluidic device, oxidation mechanism of L-ascorbic acid in the presence of free radicals, plots showing tunable shell thickness, and L-ascorbic acid (PDF)

■ AUTHOR INFORMATION

Corresponding Authors

Sei-Jung Lee − *Department of Pharmaceutical Engineering, Daegu Haany University, Gyeongsan, Gyeongbuk 38610, Korea*; Email: sjlee@dhu.ac.kr

Hyomin Lee − *Department of Chemical Engineering, Pohang University of Science and Technology (POSTECH), Pohang, Gyeongbuk 37673, Korea*; orcid.org/0000-0002-0968-431X; Email: hyomin@postech.ac.kr

Chang-Hyung Choi − *Division of Cosmetic Science and Technology, Daegu Haany University, Gyeongsan, Gyeongbuk 38610, Korea*; orcid.org/0000-0002-7561-3720; Email: cchoi@dhu.ac.kr

Authors

Jin-Ok Chu − *Division of Cosmetic Science and Technology, Daegu Haany University, Gyeongsan, Gyeongbuk 38610, Korea*

Yoon Choi − *Division of Cosmetic Science and Technology, Daegu Haany University, Gyeongsan, Gyeongbuk 38610, Korea*

Do-Wan Kim − *Department of Pharmaceutical Engineering, Daegu Haany University, Gyeongsan, Gyeongbuk 38610, Korea*

Hye-Seon Jeong − *Division of Cosmetic Science and Technology, Daegu Haany University, Gyeongsan, Gyeongbuk 38610, Korea*

Jong Pil Park − *Department of Food Science and Technology, Chung-Ang University, Anseong 17546, Korea*; orcid.org/0000-0002-4119-1574

David A. Weitz − *John A. Paulson School of Engineering and Applied Sciences and Department of Physics, Harvard University, Cambridge, Massachusetts 02138, United States*; orcid.org/0000-0001-6678-5208

Complete contact information is available at: https://pubs.acs.org/10.1021/acsami.1c20748

Author Contributions

The manuscript was written through contributions of all authors. All authors have given approval to the final version of the manuscript. J.-O.C. and Y.C. contributed equally.

https://doi.org/10.1021/acsami.1c20748
ACS Appl. Mater. Interfaces 2022, 14, 2597−2604

Notes

The authors declare no competing financial interest.

■ ACKNOWLEDGMENTS

We gratefully acknowledge partial financial support by the National Research Foundation of Korea (NRF) grant funded by the Korea government (MSIT) (No. 2021R1F1A1056481), the National Research Foundation (NRF) of Korea grant funded by the Korean government (No. 2020R1C1C1004642), the National Research Foundation of Korea (NRF) grant funded by the Korea government (MSIT) (No. 2021R1A4A1022206), and the National Research Foundation of Korea (NRF) grant funded by the Korea government (MSIT) (No. 2019R1A2C1088927). The work at Harvard University was supported in part by the NSF through the Harvard MRSEC (DMR-2011754).

■ ABBREVIATIONS

ROS, reactive oxygen species
L-AA, L-ascorbic acid
α-T, α-tocopherol
Ca-EDTA, calcium disodium EDTA
CM-H_2DCFDA, chloromethyl derivative of H_2DCFDA

■ REFERENCES

(1) Xu, C.; Hu, S.; Chen, X. Artificial Cells: From Basic Science to Applications. *Mater. Today* **2016**, *19*, 516−532.
(2) Apel, K.; Hirt, H. Reactive Oxygen Species: Metabolism, Oxidative Stress, and Signal Transduction. *Annu. Rev. Plant Biol.* **2004**, *55*, 373−399.
(3) Forman, H. J.; Zhang, H. Targeting Oxidative Stress in Disease: Promise and Limitations of Antioxidant Therapy. *Nat. Rev. Drug Discovery* **2021**, *20*, 689−709.
(4) Kamiya, K.; Takeuchi, S. Giant Liposome Formation toward the Synthesis of Well-Defined Artificial Cells. *J. Mater. Chem. B* **2017**, *5*, 5911−5923.
(5) Shohda, K.-i.; Sugawara, T. DNA Polymerization on the Inner Surface of a Giant Liposome for Synthesizing an Artificial Cell Model. *Soft Matter* **2006**, *2*, 402−408.
(6) Yuan, W.; Piao, J.; Dong, Y. Advancements in the Preparation Methods of Artificial Cell Membranes with Lipids. *Mater. Chem. Front.* **2021**, *5*, 5233−5246.
(7) Podolsky, K. A.; Devaraj, N. K. Synthesis of Lipid Membranes for Artificial Cells. *Nat. Rev. Chem.* **2021**, *5*, 676−694.
(8) Buddingh', B. C.; van Hest, J. C. M. Artificial Cells: Synthetic Compartments with Life-Like Functionality and Adaptivity. *Acc. Chem. Res.* **2017**, *50*, 769−777.
(9) Shum, H. C.; Kim, J.-W.; Weitz, D. A. Microfluidic Fabrication of Monodisperse Biocompatible and Biodegradable Polymersomes with Controlled Permeability. *J. Am. Chem. Soc.* **2008**, *130*, 9543−9549.
(10) Kim, S.-H.; Kim, J. W.; Kim, D.-H.; Han, S.-H.; Weitz, D. A. Polymersomes Containing a Hydrogel Network for High Stability and Controlled Release. *Small* **2013**, *9*, 124−131.
(11) Amstad, E.; Kim, S.-H.; Weitz, D. A. Photo- and Thermoresponsive Polymersomes for Triggered Release. *Angew. Chem., Int. Ed.* **2012**, *51*, 12499−12503.
(12) Weiss, M.; Frohnmayer, J. P.; Benk, L. T.; Haller, B.; Janiesch, J.-W.; Heitkamp, T.; Börsch, M.; Lira, R. B.; Dimova, R.; Lipowsky, R.; Bodenschatz, E.; Baret, J.-C.; Vidakovic-Koch, T.; Sundmacher, K.; Platzman, I.; Spatz, J. P. Sequential Bottom-up Assembly of Mechanically Stabilized Synthetic Cells by Microfluidics. *Nat. Mater.* **2018**, *17*, 89−96.
(13) Deng, N.-N.; Yelleswarapu, M.; Huck, W. T. S. Monodisperse Uni- and Multicompartment Liposomes. *J. Am. Chem. Soc.* **2016**, *138*, 7584−7591.
(14) Choi, C.-H.; Wang, H.; Lee, H.; Kim, J. H.; Zhang, L.; Mao, A.; Mooney, D. J.; Weitz, D. A. One-Step Generation of Cell-Laden Microgels Using Double Emulsion Drops with a Sacrificial Ultra-Thin Oil Shell. *Lab Chip* **2016**, *16*, 1549−1555.
(15) Utech, S.; Prodanovic, R.; Mao, A. S.; Ostafe, R.; Mooney, D. J.; Weitz, D. A. Microfluidic Generation of Monodisperse, Structurally Homogeneous Alginate Microgels for Cell Encapsulation and 3d Cell Culture. *Adv. Healthcare Mater.* **2015**, *4*, 1628−1633.
(16) Tan, H.; Guo, S.; Dinh, N.-D.; Luo, R.; Jin, L.; Chen, C.-H. Heterogeneous Multi-Compartmental Hydrogel Particles as Synthetic Cells for Incompatible Tandem Reactions. *Nat. Commun.* **2017**, *8*, 663.
(17) Seiffert, S.; Thiele, J.; Abate, A. R.; Weitz, D. A. Smart Microgel Capsules from Macromolecular Precursors. *J. Am. Chem. Soc.* **2010**, *132*, 6606−6609.
(18) Liu, E. Y.; Choi, Y.; Yi, H.; Choi, C.-H. Triple Emulsion-Based Rapid Microfluidic Production of Core−Shell Hydrogel Microspheres for Programmable Biomolecular Conjugation. *ACS Appl. Mater. Interfaces* **2021**, *13*, 11579−11587.
(19) Li, W.; Zhang, L.; Ge, X.; Xu, B.; Zhang, W.; Qu, L.; Choi, C.-H.; Xu, J.; Zhang, A.; Lee, H.; Weitz, D. A. Microfluidic Fabrication of Microparticles for Biomedical Applications. *Chem. Soc. Rev.* **2018**, *47*, 5646−5683.
(20) Lee, T. Y.; Choi, T. M.; Shim, T. S.; Frijns, R. A. M.; Kim, S.-H. Microfluidic Production of Multiple Emulsions and Functional Microcapsules. *Lab Chip* **2016**, *16*, 3415−3440.
(21) Lee, M. H.; Hribar, K. C.; Brugarolas, T.; Kamat, N. P.; Burdick, J. A.; Lee, D. Harnessing Interfacial Phenomena to Program the Release Properties of Hollow Microcapsules. *Adv. Funct. Mater.* **2012**, *22*, 131−138.
(22) Abbaspourrad, A.; Carroll, N. J.; Kim, S.-H.; Weitz, D. A. Polymer Microcapsules with Programmable Active Release. *J. Am. Chem. Soc.* **2013**, *135*, 7744−7750.
(23) Windbergs, M.; Zhao, Y.; Heyman, J.; Weitz, D. A. Biodegradable Core−Shell Carriers for Simultaneous Encapsulation of Synergistic Actives. *J. Am. Chem. Soc.* **2013**, *135*, 7933−7937.
(24) Choi, C.-H.; Weitz, D. A.; Lee, C.-S. One Step Formation of Controllable Complex Emulsions: From Functional Particles to Simultaneous Encapsulation of Hydrophilic and Hydrophobic Agents into Desired Position. *Adv. Mater.* **2013**, *25*, 2536−2541.
(25) Xu, W.; Ledin, P. A.; Iatridi, Z.; Tsitsilianis, C.; Tsukruk, V. V. Multicompartmental Microcapsules with Orthogonal Programmable Two-Way Sequencing of Hydrophobic and Hydrophilic Cargo Release. *Angew. Chem., Int. Ed.* **2016**, *55*, 4908−4913.
(26) Arriaga, L. R.; Datta, S. S.; Kim, S.-H.; Amstad, E.; Kodger, T. E.; Monroy, F.; Weitz, D. A. Ultrathin Shell Double Emulsion Templated Giant Unilamellar Lipid Vesicles with Controlled Microdomain Formation. *Small* **2014**, *10*, 950−956.
(27) Kim, S.-H.; Kim, J. W.; Cho, J.-C.; Weitz, D. A. Double-Emulsion Drops with Ultra-Thin Shells for Capsule Templates. *Lab Chip* **2011**, *11*, 3162−3166.
(28) Deng, N.-N.; Vibhute, M. A.; Zheng, L.; Zhao, H.; Yelleswarapu, M.; Huck, W. T. S. Macromolecularly Crowded Protocells from Reversibly Shrinking Monodisperse Liposomes. *J. Am. Chem. Soc.* **2018**, *140*, 7399−7402.
(29) Deshpande, S.; Brandenburg, F.; Lau, A.; Last, M. G. F.; Spoelstra, W. K.; Reese, L.; Wunnava, S.; Dogterom, M.; Dekker, C. Spatiotemporal Control of Coacervate Formation within Liposomes. *Nat. Commun.* **2019**, *10*, 1800.
(30) Choi, C.-H.; Lee, H.; Abbaspourrad, A.; Kim, J. H.; Fan, J.; Caggioni, M.; Wesner, C.; Zhu, T.; Weitz, D. A. Triple Emulsion Drops with an Ultrathin Water Layer: High Encapsulation Efficiency and Enhanced Cargo Retention in Microcapsules. *Adv. Mater.* **2016**, *28*, 3340−3344.
(31) Lee, H.; Choi, C.-H.; Abbaspourrad, A.; Wesner, C.; Caggioni, M.; Zhu, T.; Nawar, S.; Weitz, D. A. Fluorocarbon Oil Reinforced Triple Emulsion Drops. *Adv. Mater.* **2016**, *28*, 8425−8430.
(32) Jeong, H.-S.; Kim, E.; Nam, C.; Choi, Y.; Lee, Y.-J.; Weitz, D. A.; Lee, H.; Choi, C.-H. Hydrogel Microcapsules with a Thin Oil

https://doi.org/10.1021/acsami.1c20748
ACS Appl. Mater. Interfaces 2022, 14, 2597−2604

Layer: Smart Triggered Release Via Diverse Stimuli. *Adv. Funct. Mater.* **2021**, *31*, No. 2009553.
(33) Lee, S.; Che, B.; Tai, M.; Li, W.; Kim, S. H. Designing Semipermeable Hydrogel Shells with Controlled Thickness through Internal Osmosis in Triple-Emulsion Droplets. *Adv. Funct. Mater.* **2021**, *31*, No. 2105477.
(34) Choe, E.; Min, D. B. Mechanisms of Antioxidants in the Oxidation of Foods. *Compr. Rev. Food Sci. Food Saf.* **2009**, *8*, 345−358.
(35) Gallarate, M.; Carlotti, M. E.; Trotta, M.; Bovo, S. On the Stability of Ascorbic Acid in Emulsified Systems for Topical and Cosmetic Use. *Int. J. Pharm.* **1999**, *188*, 233−241.
(36) Franke, A. A.; Murphy, S. P.; Lacey, R.; Custer, L. J. Tocopherol and Tocotrienol Levels of Foods Consumed in Hawaii. *J. Agric. Food Chem.* **2007**, *55*, 769−778.
(37) Zhang, L.; Chen, K.; Zhang, H.; Pang, B.; Choi, C.-H.; Mao, A. S.; Liao, H.; Utech, S.; Mooney, D. J.; Wang, H.; Weitz, D. A. Microfluidic Templated Multicompartment Microgels for 3d Encapsulation and Pairing of Single Cells. *Small* **2018**, *14*, No. 1702955.
(38) Lee, K. Y.; Mooney, D. J. Alginate: Properties and Biomedical Applications. *Prog. Polym. Sci.* **2012**, *37*, 106−126.
(39) Robinson, D.; Anderson, J. E.; Lin, J. L. Measurement of Diffusion Coefficients of Some Indoles and Ascorbic Acid by Flow Injection Analysis. *Am. J. Phys. Chem.* **1990**, *94*, 1003−1005.
(40) Adem, S. M.; Leung, S. H.; Sharpe Elles, L. M.; Shaver, L. A. A Laboratory Experiment for Rapid Determination of the Stability of Vitamin C. *J. Chem. Educ.* **2016**, *93*, 1766−1769.
(41) Kong, L.; Chen, R.; Wang, X.; Zhao, C.-X.; Chen, Q.; Hai, M.; Chen, D.; Yang, Z.; Weitz, D. A. Controlled Co-Precipitation of Biocompatible Colorant-Loaded Nanoparticles by Microfluidics for Natural Color Drinks. *Lab Chip* **2019**, *19*, 2089−2095.
(42) Wu, B.; Yang, C.; Li, B.; Feng, L.; Hai, M.; Zhao, C.-X.; Chen, D.; Liu, K.; Weitz, D. A. Active Encapsulation in Biocompatible Nanocapsules. *Small* **2020**, *16*, No. 2002716.
(43) Nisisako, T. Microstructured Devices for Preparing Controlled Multiple Emulsions. *Chem. Eng. Technol.* **2008**, *31*, 1091−1098.
(44) Klimczak, I.; Małecka, M.; Szlachta, M.; Gliszczyńska-Świgło, A. Effect of Storage on the Content of Polyphenols, Vitamin C and the Antioxidant Activity of Orange Juices. *J. Food Compos. Anal.* **2007**, *20*, 313−322.

https://doi.org/10.1021/acsami.1c20748
ACS Appl. Mater. Interfaces 2022, 14, 2597−2604